

Short Communication

Comparison of Electrochemical Noise (EN) Signal And Corrosion Products Signal Image of Ti-6Al-4V

C.G. Nava-Dino^{1, 2}, G. López-Ocaña³, J. A. Cabral-Miramontes⁴, M.A. Luna-Ramirez⁵,
H. Monreal-Romero⁶, R. Bautista-Margulis³, J.G. Chacon-Nava¹, A. Martinez-Villafañe^{1,*}

¹ Departamento de Integridad y Diseño de Materiales Compuestos/Grupo Corrosión. Centro de Investigación en Materiales Avanzados. S.C. CIMAV. Miguel de Cervantes No 120 Complejo Industrial Chihuahua, C.P 31109, Chihuahua, Chih. México.

² Universidad Autónoma de Chihuahua, Facultad de Ingeniería. Chihuahua, Circuito No 1., Campus Universitario 2 Chihuahua, Chih. C.P. 31125, México. Tel 614-4-42-95-07

³ Universidad Juárez Autónoma de Tabasco, División Académica de Ciencias Biológicas, Villahermosa-Tabasco, C.P. 86040. México.

⁴ Cinvestav-Querétaro Libramiento Norponiente 2000 Fracc. Real de Juriquilla 76230 Querétaro, Qro., México.

⁵ Instituto de Investigaciones Eléctricas, Av. Reforma 113, Col. Palmira, 62490-Cuernavaca, Morelos, México.

⁶ Universidad Autónoma de Chihuahua, Facultad de Odontología, Chihuahua, Chih. México.

*E-mail: martinez.villafañe@cimav.edu.mx

Received: 3 July 2012 / Accepted: 29 September 2012 / Published: 1 November 2012

Electrochemical noise (EN) measurements and their corrosion products were observed by Scanning Electron Microscopy (SEM). Digital image process allows changing the image result of corrosion products in an equivalent signal. Samples of Ti-6Al-4V were produced by mechanical milling at different milling times. After that, they are sintering by SPS (Spark Plasma Sintering) to predict the behavior of the samples in Hank's solution. The images obtained by SEM were changed to binary map and then changed to a two-dimensional array. SEM images showed the surface topography of corrosion products.

Keywords: Microstructure, SPS, Electrochemical noise, Image processing, Signal processing.

1. INTRODUCTION

Ti6Al4V has been also used preferentially in orthopedic replacement due to its added mechanical strength. Titanium forms a biocompatible surface oxide layer capable of interacting with surrounding biological fluids [1-2]. Also Ti alloys, such as Ti-6Al-4V, has been considered one of the

most commonly materials used as implants in large surfaces and has been created using several techniques. Fabrication of porous implants with coatings, usually involves SPS (Spark Plasma Sintering) or powder sintering in a solid substrate. The common way to handle powder metallurgy consists in compact samples of material and then sintering at high temperatures. Reactive materials like Ti need to be handled under inert atmospheres. High temperature and compactation produce changes in microstructure and mechanical properties [3]. Most surfaces, in natural or human-made systems can be characterized with digital image processing [4].

1.1 Image Processing

Image processing has been a good tool to analyze and understand the behavior of several samples in industrial and medical areas. Medical images allow identify certain anatomical structures. This images after they are analyzed by an algorithm of digital images, identify a region of the image as a ROI (Region-of-interest). Some medical applications need to change objects on the region of interest, keeping their topography. Several authors connect every part of the topography surfaces with images and numbers [5-6]. In this research milling process, an SPS shows different changes in sample surfaces, bearing in mind to be focused in a ROI, which shows notable differences. Also, Digital Image Correlation (DIC) provides deformation information of a specimen by processing two digital images that are captured before and after the deformation. On using the discrete pixels of a digital image and their grey level values for intensity, these data are recorded as a two-dimensional array [7-8]. Another way to find information in images consist in applying algorithms of detection and segmentation [9].

1.2. Eletrochemical characterization

The electrode of Ti-6Al-4V was coated with epoxy resin and then was rinsed in Hank's solution. The Hank's solution has a chemical composition (in g/l) 8 NaCl, 0.14 CaCl₂, 0.4 KCl, 0.35 NaHCO₃, 1Glucose, 0.1 NaH₂PO₄, 0.1 MgCl₂.6H₂O, 0.06 Na₂HPO₄.2H₂O y 0.06 MgSO₄.7H₂O to distilled water [10-11]. Samples were immersed in Hank's solution for half an hour for stabilization and the open circuit potential was measured during this period with a multimeter; the OCP samples were -279 and -189 mV vs SCE for 0 to 8 h milling time and then sintering by SPS. All tests were performed at ± 37 °C; this temperature was used to simulate human body temperature. Analysis was done according to ASTM G199.

2. MATERIALS AND METHODS

2.1 Materials and experimental procedure

Pure materials (Alfa Aesar): titanium (99.5% purity), aluminum (99.5%), vanadium (99.5%) powders. The first step was the preparation by milling with the corresponding quantity of metal

powder in a high energy SPEX 8000M connected to a hardened steel container with 13 mm(\emptyset) balls as milling media and an inert Ar atmosphere.

Pressed samples were mounted, polished and etched using standard metallographic techniques in order to carry out the microstructural observations by using a scanning electron microscope JEOL-5800-LV. Sintering process was made by SPS (Spark Plasma Sintering); during SPS, a pulsed current generates plasma which leads to a surface activation of the powder particles.

3. RESULTS AND DISCUSSION

Electrochemical noise (EN), knew as spontaneous fluctuations of the electrical quantities. Where, these fluctuations manifest in the form of potential and current noise signals during different corrosion processes and appear to be connected to local variations in the rates of anodic and cathodic reactions as a consequence of both stochastic processes (breakdown and repassivation of the passive film) and deterministic processes (film formation and pit propagation)[12]. Using titanium as a sample, coating TiO₂ oxidized layer helps to protect another material samples as a steel 304 under Hank's solution immersion conditions [13]. In this research the spectral analysis of the correlated current and potential noise data record (2048 points) was obtained from Ti-6Al-4V SPS sintering powders electrode.

Table 1. Electrochemical noise (EN) of Ti-6Al-4V

Specimen Ti-6Al-4V	R _n (ohm.cm ²)	Localization Index IL	Corrosion Type
SPS 0h	29596.099	0.6658104	Located
SPS 3h	95659.255	0.61214846	Located
SPS 5h	10200.137	0.55714585	Located
SPS 8h	12912.730	0.46640928	Located

Table 1 shows the results of EN analysis, where is appreciable that corrosion samples are located in all the cases, this mean independently of milling hours the corrosion type is located. These results could be compared with other researches whose use artificial saliva (commonly referred as Fusayama Meyer solution) with saturated calomel electrode (SCE) as this research, but the values obtained looks higher than those found in the current research, since they were around (-586 to -470mV vs. SCE)[14].

To understand the results from EN analysis, a traditional tool that provides this transformation is the fast Fourier transform (FFT) algorithm, which performs a spectral analysis of the random transients of the EN signal [15-16]. Another way to analyze the signal obtained consists in study the structure of the EN time record in the time domain and described by the Hurst exponent H [17]. In figure 1 (EN) signal of Ti-6Al-4V 3h in Hank's solution was observed, the behavior of the samples showed good resistance of corrosive environment. This means that, the passivity breakdown on metal

surfaces in the different milling hours were similar. In figure 2 the signal of 0h, 3h, 5h and 8h was also observed. In 5h the fluctuation of the signal was originated by a located pitting. Concerning the behavior of the samples, some researchers are referred to “nanoelectrochemistry”, to measure the potential or current transients recorded as a function of time to know whether or not exist the pit initiation processes [18].

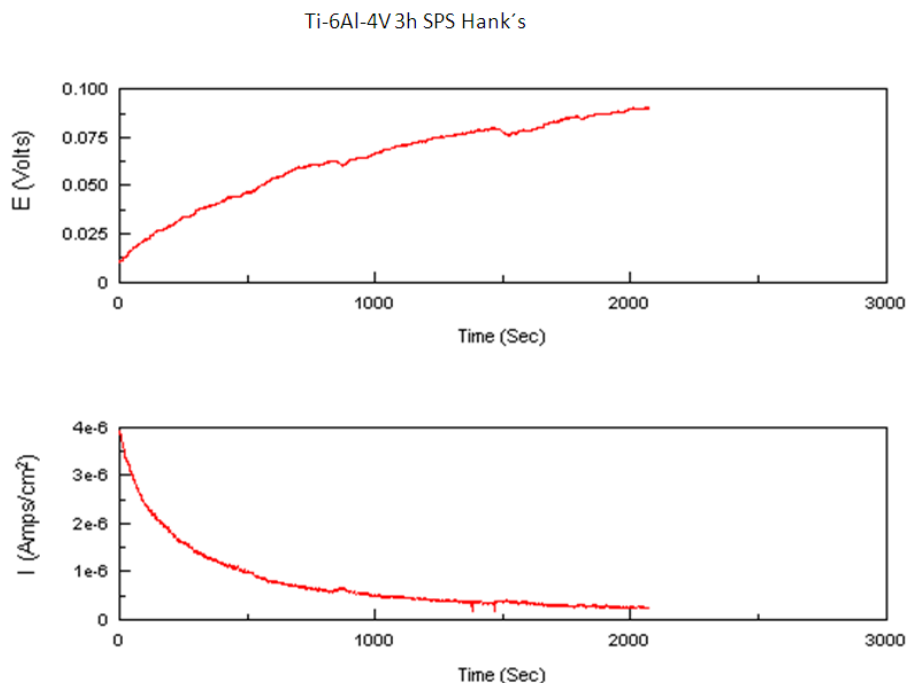


Figure 1. Electrochemical noise (EN), of Ti-6Al-4V in Hank's solution

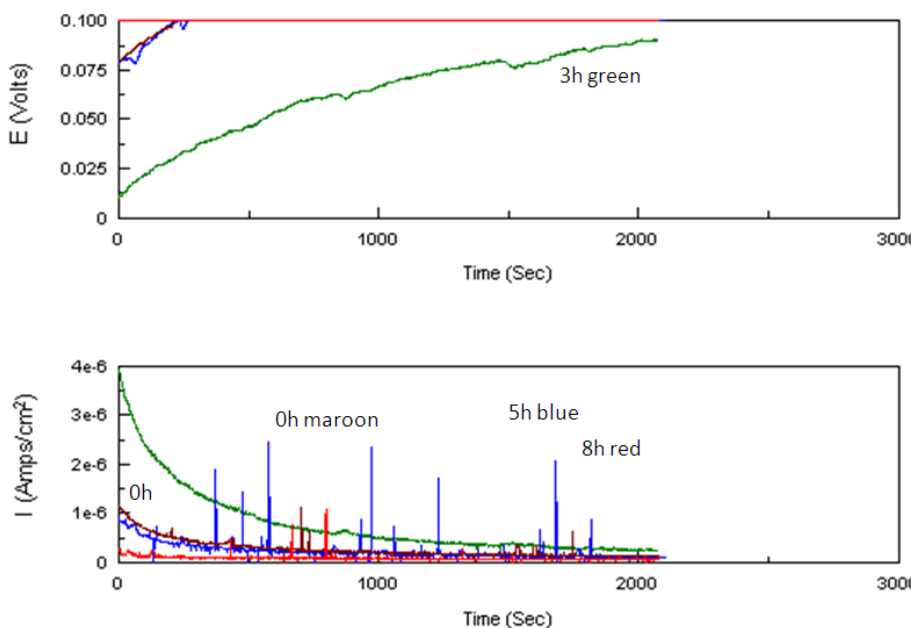


Figure 2. EN signals of 0h, 3h, 5h and 8h milling time with SPS sintering.

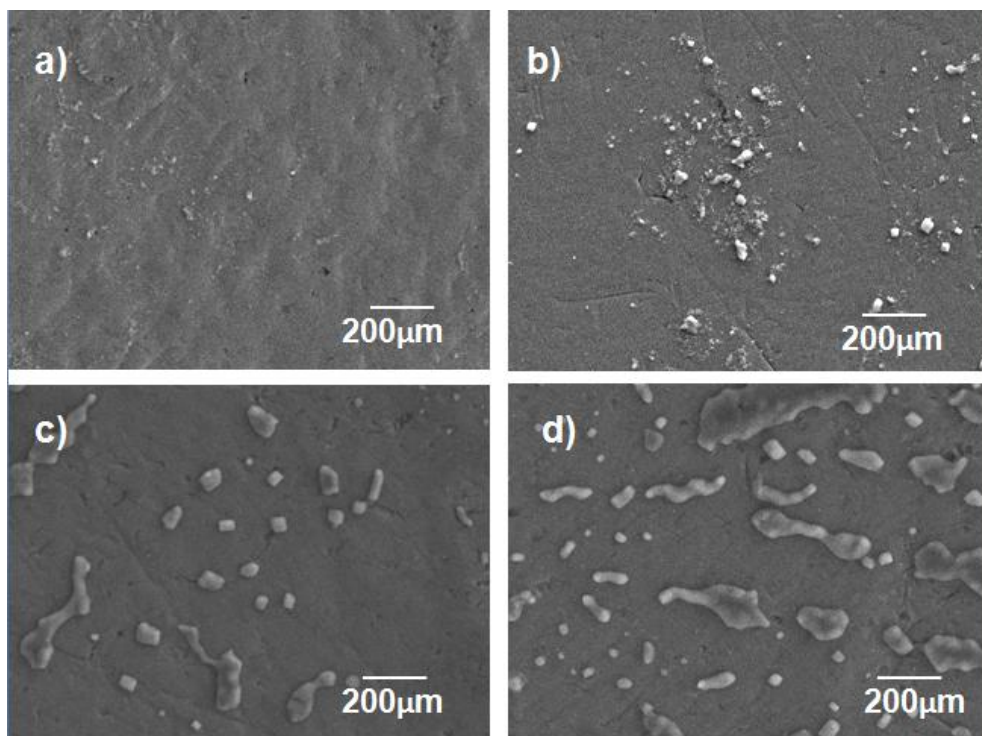


Figure 3. Corrosion products of Ti-6Al-4V under Hank’s solution, a) 0h milling time and sintering SPS, b) 3h, c) 5h, d) 8h.

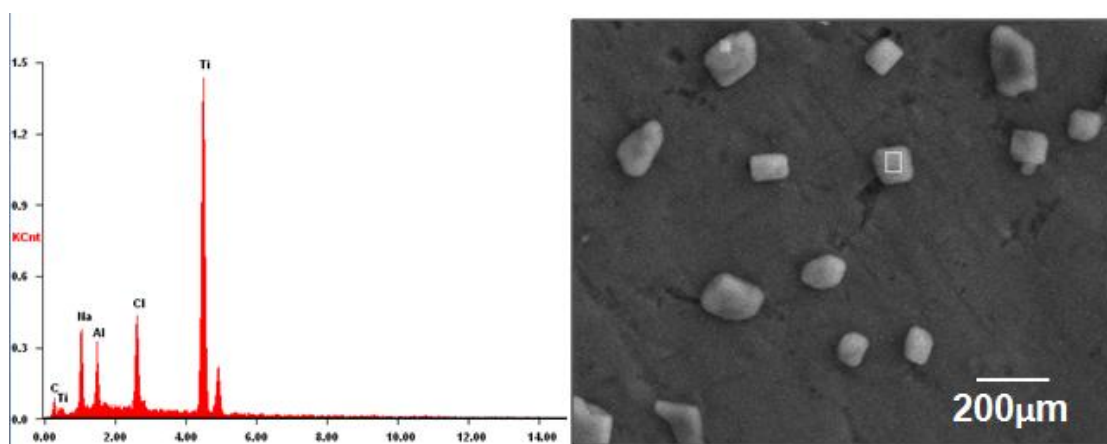


Figure 4. Analysis of corrosion products showed by EDS analysis

In this research, the microstructure of material was analyzed by digital imaging process as well as the typical ways to characterize materials. The images obtained from SEM as a result of test electrochemical noise can be observed in figure 3. In these images the corrosion products were observed with some periodical behavior. The digital process of the images using Matlab, permits observe the most important or remarkable points of the image. These points were connected by a line that is a drawing in the image. As a reference to analyze the images with Matlab, some studies about geological rocks process the SEM images using Adobe Photoshop and Image SXM. For the D-mapping technique, a single bitmap separating all grains from the matrix was required. Using software,

a number of segmentation techniques were tested and the results compared visually. The best results were obtained by observing both the image and the grey value histogram during grey level slicing or thresholding [19]. Applying algorithms to dimensioning images has a seemingly universal applicability.

The results from digital image process were done under principles of morphological operations to delimit the important regions in micrographs. In the figure 4 corrosion products and EDS analysis is observed, then the images from SEM from 0h to 8h and sintering were done dimensioning their micrographs to a matrix and then taking the information to create the signal, in Fig 5 the original images from SEM and then changed as a signal are presented. Thus SEM images were in their vertical and horizontal positions and then developed by Matlab software. Hence to obtain borders of the image allows analyze the surface of the image; the morphology of the image can then be identified by dimension [20].

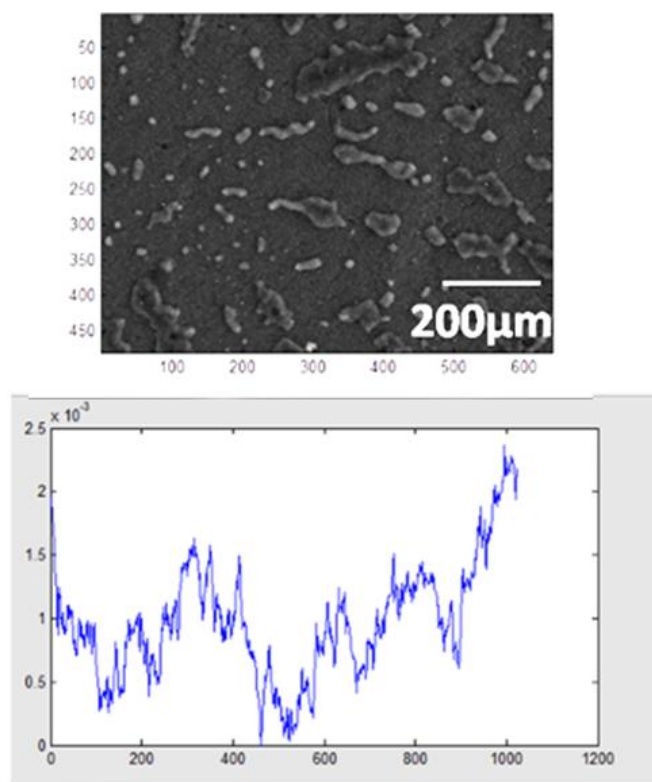


Figure 5. Image of corrosion products showed with their corresponding signal.

Corrosion products make distinctive features into the surface of the material. Another way to handle the contour of images is using Fourier Transform [21]. Using micrographs, as a result of electrochemical test; the signal aids at understanding the behaviour of the material. This result helps to improve the alloying to be used in several applications because it is possible to understand the surface and predict their behaviour. Other studies modeling work on microstructure, properties and applications of titanium alloys using DEFORM software or ANSYS software to understand titanium

behavior [22-23]. Connect the corrosion image with an equivalent signal was a process made to count the pitting corrosion in terms of metal loss, where the derived phase congruency map is further used as the initial contour for a segmentation algorithm using local binary fitting (LBF), to characterize the pitting corrosion, signal features need to be extracted from the thermography inspection data in some studies [24-25].

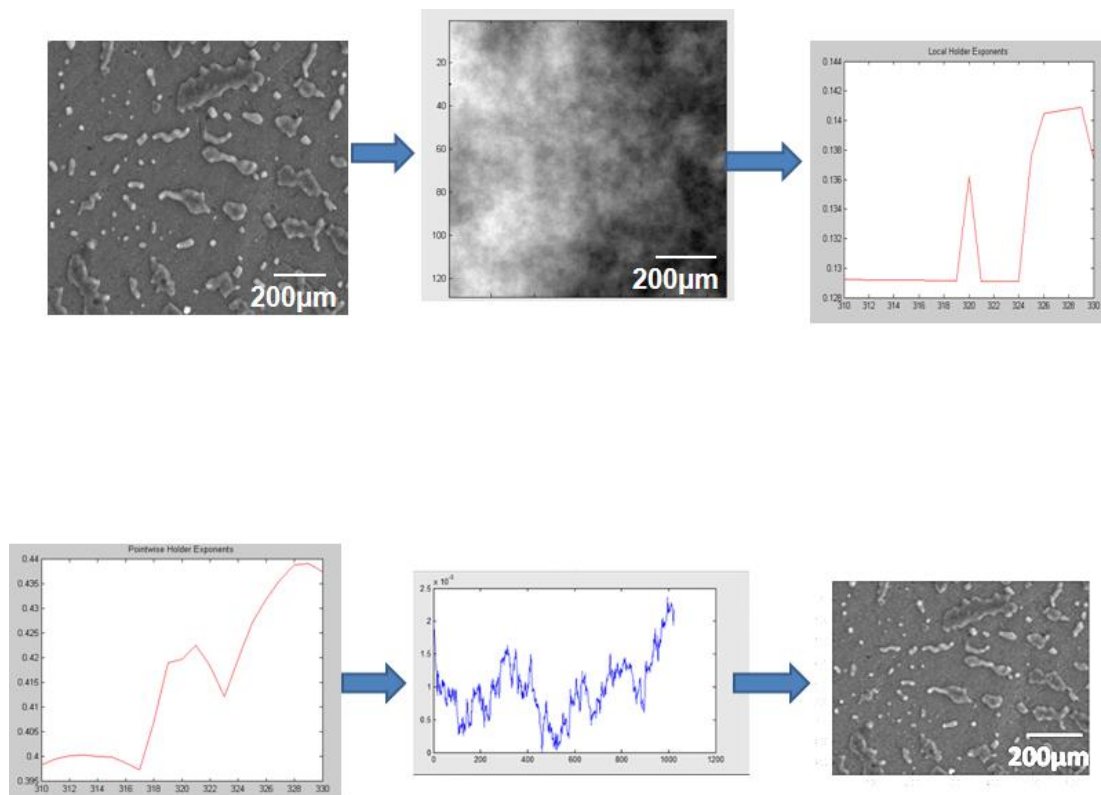


Figure 6. Processing the image of corrosion products.

The comparisons of SEM images by other studies were converted into binary images also to analyze it [26]. When the binary image is obtained, the next step is to show the signal that is calculated using Hölder exponents. There are many ways to measure the local regularity of a signal. One of them is the use of pointwise Hölder exponent [27]. Hölder exponents also have been used to analyze time series signals [28]; in this research the principal signals have been made as a time series signals. The figure 6 shows the image result of EN test and the processing to gray scale until the signal is reached.

4. CONCLUSIONS

- Matlab software was used to handle corrosion images obtained from SEM test, in order to analyze the corrosion products of the material dimensioning the images to determine the behavior of the material.

- The samples of Ti-6Al-4V to 0, 3, 5 and 8 h of milling time have different structural shapes on the surface; those differences were appreciated in the reduction of particle size and grain as milling time increases.
- The rupture of the passivating oxide film induced by the ions, describe nucleation of corrosion producing pitting in the sample.
- The sequence of current spikes in the anodic direction only are due to transient breakdown of passivity layer observed in the results of EN commonly used in “located” corrosion, that is the corrosion type found in the current investigation.
- The comparison between the values of the Hölder exponents in a signal and the EN experimental signals leads to the conclusion that the signals obtained by image of corrosion products are quite similar to those obtained from the EN experimental signal.

ACKNOWLEDGMENTS

This research work was supported by Nanomining-263942 (FP7-NMP-2010-EU-MEXICO). The technical assistance by Victor Orozco, Karla Campos, Adan Borunda-Terrazas, Jair Lugo Cuevas is gratefully acknowledged.

References

1. D.E. MacDonald, B.E. Rapuanod, N. Deoa, M. Stranickc, P. Somasundarana, A.L. Boskey, *Biomaterials* 25 (2004) 3135-3146.
2. G. Lutjering, J.C. Williams, Springer, 2007.
3. W.H. Lee, C.Y. Hyun, *J Mater Process Tech* 189 (2007) 219–223.
4. L. M.F. Ribeiro, A. Horovistiz, G. A. Jesuino, L. de O. Hein, N. P. Abbade, S. J. Crnkovic, *Mater Lett*, 56 (2002) 512-517.
5. W. Birkfellner, CRC Press, 2011.
6. C. Lohou, G. Bertrand, *Pattern Recogn*, 40 (2007) 2301-2314.
7. S. Hwang, J. Horn, H.Jiun Wang, *Opt Lasers Eng* 46 (2008) 281–289.
8. Y. Chen, W. qiJin, LeiZhao, F.wenLi, *Optik* 120 (2009) 835–844
9. A. Oliver , J. Freixenet, J. Marti , E. Perez , J. Pont , E. Denton, R. Zwiggelaar, *Med Image Anal* 14 (2010) 87–110
10. C. Yuyong, W. Xiaopeng, X. Lijuan, L. Zhiguang, K. Woo, *J mech behav biomed*, (2012),97-107.
11. X. Shi, L. Xu, Q. Wang, *Surf Coat Tech* 205 (2010) 1730–1735
12. M. G. Pujar, T. Anita, H. Shaikh, R. K. Dayal and H. S. Khatak, *Int. J. Electrochem. Sci.*, 2 (2007) 301 - 310
13. F. Barragán, R. Guardián, C. Menchaca, I. Rosales, J. Uruchurtu, *Int. J. Electrochem. Sci.*, 5 (2010) 1799 – 1809
14. B. Sivakumar, S. Kumar, T. Narayanan, *Wear* 270 (2011) 317–324
15. C. Valentini, J. Fiora, G. Ybarra, *Prog Org Coat*, 73 (2012) 173-177
16. D. Xia, S. Song, J. Wang, J. Shi, H. Bi, Z. Gao, *Electrochem Commun*, 15(2012), 88-92
17. E. Sarmiento, J. G. González-Rodríguez, J. Uruchurtu, O.Sarmiento, M. Menchaca, *Int. J. Electrochem. Sci.*, 4 (2009) 144 - 155
18. G.T. Burstein, M. Carboneras, B.T. Daymond, *Electrochim Acta* 55 (2010) 7860–7866
19. R. Heilbronner, N. Keulen, *Tectonophysics* 427 (2006) 199–216.
20. D. Baumer, S. Versick, B. Vogel, *Atmos Environ* 42 (2008) 2593–2602
21. J.B. Florindo, O.M. Bruno, *Chaos, Soliton Fract* 44 (2011) 851–861

22. Q. Zhao, G. Wu, W. Sha, *Comp Mater Sci* 50 (2010) 516–526
23. B. Sabuncuoglu, S. Dag, B. Yildirim, *Comp Mater Sci* 52 (2012) 246–252
24. Z. Liu, MarcGenest, DennisKry, *NDT&E Int* 47 (2012) 105–115
25. R. Pidaparti, B. Aghazadeh, A. Whitfield, A.S. Rao, G. Mercier, *Corros Sci* 52 (2010) 3661–3666
26. Y. Wu, Q. Lin, Z. Chen, W. Wu, H. Xiao, *J Food Eng* 109 (2012) 182–187
27. B. Buard, A. Humeau, D. Rousseau , F. Chapeau-Blondeau , P. Abraham, *IRBM* 31 (2010) 175–181
28. S.J. Loutridis, An algorithm for the characterization of time-series based on local regularity, *Physica A* 381 (2007) 383–398